Measurement 135 (2019) 189–198

Contents lists available at ScienceDirect

Measurement

journal homepage: www.elsevier.com/locate/measurement

Research on the improved method for dual foot-mounted Inertial/Magnetometer pedestrian positioning based on adaptive inequality constraints Kalman Filter algorithm

Qiuying Wang [a,*], Ming Cheng [a], Aboelmagd Noureldin [b], Zheng Guo [a]

[a] College of Information and Communication Engineering, Harbin Engineering University, Harbin, China
[b] Navigation and Instrumentation Research Group, Electrical and Computer Engineering, Royal Military College of Canada, Kingston, Canada

ARTICLE INFO

Article history:
Received 20 September 2018
Received in revised form 9 November 2018
Accepted 18 November 2018
Available online 19 November 2018

Keywords:
MIMU
Magnetometer
Pedestrian positioning
Dual foot
Adaptive inequality constraints Kalman Filter

ABSTRACT

The advantages of foot-mounted inertial pedestrian position system are passive, full-autonomous and not affected by environment. However, the disadvantage of the accumulating pedestrian position error, which is introduced by Micro Inertial Measurement Unit (MIMU) noise, limits its application. Zero Velocity Update (ZUPT) algorithm is proposed to correct the accumulating error. But ZUPT has poor performance due to the unobserved position error and azimuth misalignment angle, which results in a continuous increase in azimuth error and an increase in positioning error. To solve the problem, the improved method for dual foot-mounted Inertial/Magnetometer pedestrian positioning based on adaptive inequality constraints Kalman Filter is proposed in this paper. Our first contribution in this paper is studying the adaptive inequality constraints Kalman Filter algorithm for dual-foot inertial position algorithm. In this method, the adaptive inequality constraint is introduced in the Kalman Filter of ZUPT, and the constraints parameter can be online adaptive adjusted based on the character of pedestrian step length. Therefore, the accumulating position error can be decreased and limited in a range. As our second contribution, we propose an approach for estimating the magnetic disturbance in real time during the pedestrian walking period. After studying the observability properties of magnetic disturbance parameters, the magnetic disturbance can be estimated when the foot satisfied the conditions of static and angular motion. Then, the azimuth misalignment angle can be corrected by magnetometer during the ZUPT period. We illustrate the findings of our theoretical analysis using experiments based on the MTI-G710 MIMU. The achieved performance indicates that our proposed method can conveniently be used in consumer products.

1. Introduction

The pedestrian positioning system without Global Navigation Satellite System (GNSS) can be widely used in the firefighting, indoor navigation and army [1,2]. Especially in recent years, with the developing of Micro Inertial Measurement Unit (MIMU), pedestrian positioning system based on MIMU gets wide attention. When the MIMU is installed on the pedestrian body, the acceleration and angular velocity of the pedestrian are measured in real time. Then, the positioning (including position, velocity and attitude) is obtained by the dead reckoning algorithm [3,4]. However, the low precision and high noise of the MIMU result in accumulating positioning errors during the process of dead reckoning [5–8].

To solve the problem above, MIMU is installed on the pedestrian foot. The acceleration and angular velocity of the foot are measured in real time. One gait is defined as the time period between the instant of the foot touchdown and the instant of the same foot touchdown again. One gait is divided into two parts: swing and touch. When the foot is swing, dead reckoning is operating to calculate the position information; when the foot touches the ground, the foot velocity is zero in theory. Hence, the velocity obtained by dead reckoning is velocity error, which is used as the observation of Kalman Filter. Therefore, part of position error can be estimated and corrected. This algorithm is called Zero Velocity Update (ZUPT) [9–14].

However, not all the position error can be estimated and corrected by ZUPT. According to the state equation and the observation equation when the foot touches the ground, it is a linear time-invariant system. By means of studying the observability properties, ZUPT can correct the velocity error and horizontal misalignment angle, the unobserved position error and azimuth

* Corresponding author.
E-mail address: wangqiuying@hrbeu.edu.cn (Q. Wang).

https://doi.org/10.1016/j.measurement.2018.11.052
0263-2241/

misalignment angle results in a continuous increase in azimuth error and an increase in positioning error. It means that the position error caused by the velocity error and horizontal misalignment angle can be corrected, but the position error caused by azimuth error cannot be solved.

The azimuth misalignment angle of ZUPT can be estimated by introducing the magnetometer as an external sensor. A magnetometer is a sensor that measures the intensity of a magnetic field in local coordinate system. In theory, the foot heading can be obtained using the magnetic field strength measurement when the magnetometer is also installed on the foot. However, there is a measurement deviation due to the magnetic distribution, which makes it unable to be used as a reference for the pedestrian to estimate the azimuth misalignment angle [15–17]. Many methods are proposed to calibrate the magnetic distribution, including on-line calibration and off-line calibration [18–21]: for off-line calibration, the magnetometer should be installed on the turntable and rotated according to the setting rotating path. Then all the magnetometer distribution can be estimated and corrected. But it cannot be realized for pedestrian positioning in real time; for on-line calibration, whether the pedestrian walking can be satisfied the observability properties of magnetometer distribution parameters need further research [18–21].

The position error of ZUPT can be reduced by introducing the RFID as an external sensor. Two RFID sensors are installed on the left and right foot respectively. The relative position, which is measured by two RFIDs, is introduced as a new observation for Kalman Filter. Hence, the position error can be corrected [22–25]. The advantages of introducing RFID to pedestrian positioning system are improving the position accuracy and good real-time performance. The disadvantage is poor stability, because the relative position can only be measured when the heading of the two RFID is same with each other. It is hard for pedestrian walking [26,27]. Isaac Skog [28,29] proposes a method of introducing the inequality constraints into Kalman Filter to reduce the position error. The core idea of the algorithm is that the relative position between two feet is less than pedestrian body height. Then, the position error can greatly reduce and limited in a range. However, the value is too large for one gait and it is constant, so the setting value of the inequality constraints is inaccuracy.

To solve the problem, the improved method for dual foot-mounted Inertial/Magnetometer pedestrian positioning based on adaptive inequality constraints Kalman Filter algorithm is proposed in this paper. The paper is consisted of the following parts: section 2 shows the analysis result of the pedestrian gait, the principle of dead reckoning and ZUPT; Section 3 studies the adaptive inequality constraints Kalman Filter algorithm for dual-foot inertial position algorithm; Section 4 proposes an approach for estimating the magnetic disturbance in real time during the pedestrian walking period. The whole algorithm for pedestrian position system based on the proposed method in this paper is summarized in section 5, and the MTi-G710 is used as the test sensor to verify the principle of the proposed method in this part. The last part draws the conclusion.

2. Gait characteristic analysis and principle of pedestrian positioning

2.1. Gait characteristic analysis for dual foot

Pedestrian walking is a period motion process. One gait is defined as the period between the instant of the foot touchdown and the instant of the same foot touchdown again [30–32]. According to the gait characteristic, one gait can be divided into some phases. Fig. 1 is a schematic diagram shows every phase in one gait. Table 1 lists the definition of every phase in one gait.

According to Fig. 1 and Table 1, some characters of the dual foot related with walking law and the pedestrian position algorithm can be obtained:

Character 1 One gait can be divided into swing phase and supporting phase. The navigation information needs to be obtained by dead reckoning algorithm whether the foot is in the swing phase or supporting phase. The algorithm is described in Section 2.2.1.

Character 2 Fig. 2 shows more details of supporting phase, including standing initial phase, standing middle phase and

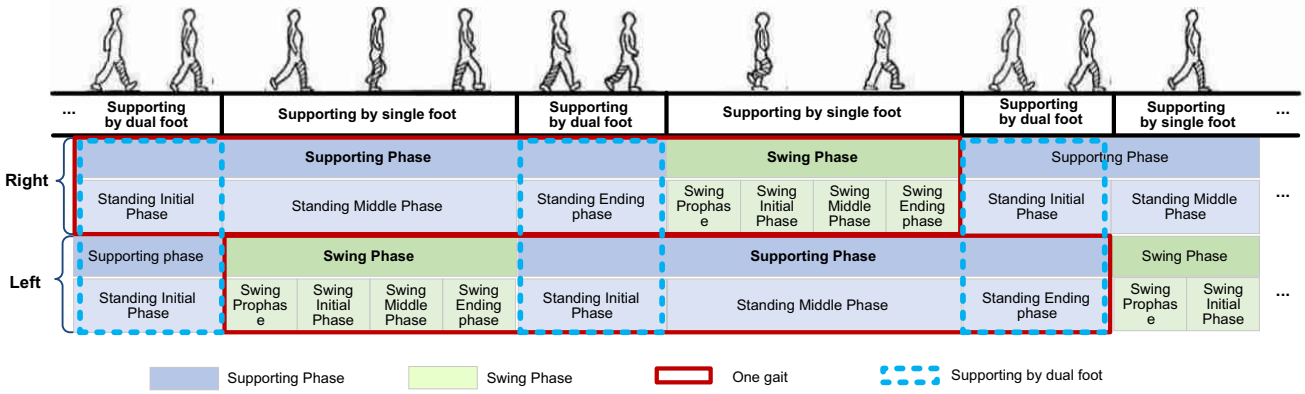

Fig. 1. Schematic diagram of every phase in one gait.

Table 1
Definition of every phase.

No.	Stage	Definition	Start Point	Ending Point
1	Standing Initial Phase	The time between the heel touch the ground for the first time and the sole touch the ground.	The heel touches the ground	The sole touch the ground
2	Standing Middle Phase	Standing on one foot	The sole touch the ground	The heel lift and leave the ground
3	Standing Ending phase	The time between the heel lift and leave the ground and the whole foot leave the ground.	The heel lift and leave the ground	The whole foot leaves the ground
4	Swing Phase	The period when the foot swing off the ground.		

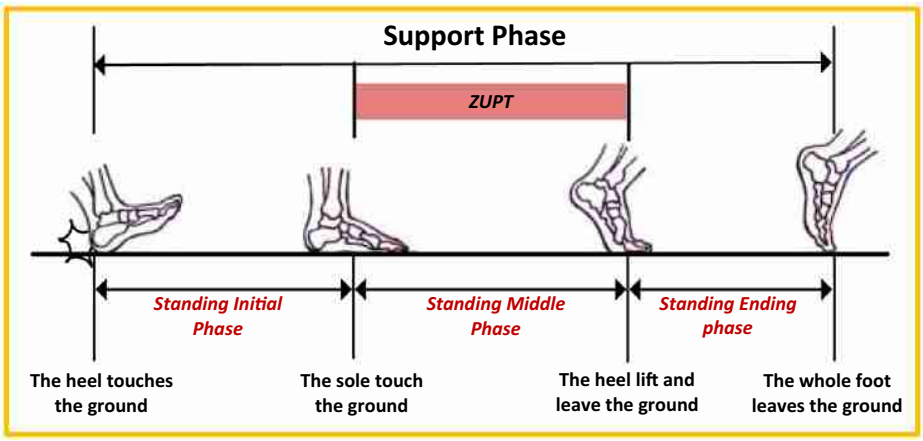

Fig. 2. Schematic diagram of supporting phase.

standing ending phase. The ZUPT algorithm is applied in the standing middle phase, during which period the foot touches the ground completely. The ZUPT algorithm is described in Section 2.2.3.

Character 3 For one gait, the instant of the heel touchdown and the toe leaves the ground are the two key information to distinguish the standing phase with the swing phase: When the toe leaves the ground, there will be a local minimum angular velocity at the x-axis, followed by a spike due to the swinging process; after the swing phase, the heel touches ground for the first time, and the angular velocity along x-axis changes from positive to negative, as shown in Fig. 3. Where, x-axis is right side, y-axis is the front, z-axis is up. Therefore, a complete gait can be divided into the standing phase and the swing phase by looking for the instant of the heel touchdown and the toe leaves the ground.

Character 4 The relative distance between the two feet is approximately constant when two feet are in the standing initial phase and in the standing ending phase respectively. The distance between the two feet changes in real time when one foot is in the standing middle phase, the other foot is in the swing phase.

2.2. Dead reckoning and basic ZUPT algorithm

2.2.1. Dead reckoning (DR) algorithm

The angular velocity and line velocity of pedestrian foot are measured by MIMU in real time, and the navigation information is obtained by dead reckoning algorithm. The core formula of dead reckoning is as follows:

$$\begin{cases} \boldsymbol{C}_{bk}^{\tilde{n}} = \boldsymbol{C}_{b(k-1)}^{\tilde{n}}(\boldsymbol{I} + \Omega_k T) \\ \boldsymbol{v}_k^{\tilde{n}} = \boldsymbol{v}_{k-1}^{\tilde{n}} + (\boldsymbol{C}_{bk}^{\tilde{n}}\boldsymbol{f}_k^b + \boldsymbol{g}^n)T \\ \boldsymbol{p}_k^{\tilde{n}} = \boldsymbol{p}_{k-1}^{\tilde{n}} + \boldsymbol{v}_k^{\tilde{n}}T + (\boldsymbol{C}_{bk}^{\tilde{n}}\boldsymbol{f}_k^b + \boldsymbol{g}^n)T^2/2 \end{cases} \quad (1)$$

where, subscripts k ($k = 1, \cdots, N$) is the sample time, b is the body system (right-front-up frame), n is the navigation coordinate frame (east-north-up frame), $\tilde{n}$ is the calculating navigation coordinate system; $\boldsymbol{C}_{bk}^{\tilde{n}}$ is the transformation matrix between b frame and $\tilde{n}$ frame at time k; $\boldsymbol{I}$ is unit matrix; T is sample time; $\boldsymbol{\Omega}_k = [\boldsymbol{\omega}_k\times]$ is antisymmetric matrix of angular velocity $\boldsymbol{\omega}_k$ measured by gyro; $\boldsymbol{v}_k^{\tilde{n}}$ is velocity along n frame at time k; $\boldsymbol{f}_k^b$ is acceleration measured by accelerometer along b frame; $\boldsymbol{g}^n = \begin{bmatrix} 0 & 0 & -g \end{bmatrix}^T$ is projection of gravity along n frame; $\boldsymbol{p}_k^{\tilde{n}}$ is calculating position result along n frame.

It can be seen from Eq. (1), measurement noise of $\boldsymbol{\omega}_k$ and $\boldsymbol{f}_k^b$ causes calculation error and finally affects the positioning accuracy. The positioning error is caused by velocity error and $\boldsymbol{C}_{bk}^{\tilde{n}}$ matrix error, and velocity error and $\boldsymbol{C}_{bk}^{\tilde{n}}$ matrix error is caused by the MIMU measurement error. Therefore, there are two ways to reduce the positioning error and improve navigation accuracy: One is to estimate and compensate the MIMU error, and eliminate the navigation error. The other is to correct the attitude error, velocity error and positioning error directly.

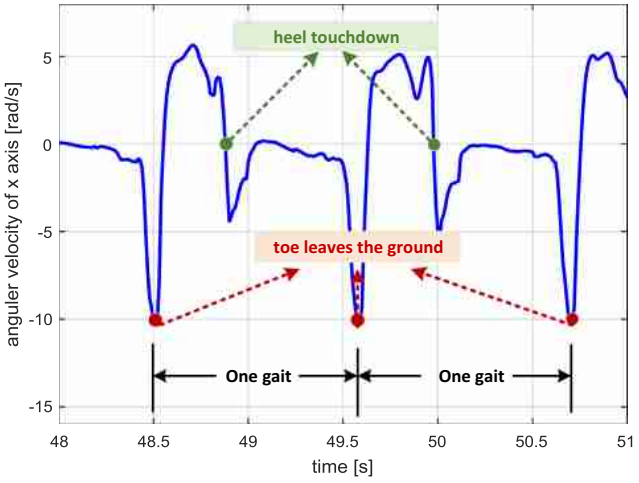

Fig. 3. Characteristic of the instant of heel touchdown and toe leaves the ground.

2.2.2. Zero velocity detection (ZVD)

According to the characteristics of the supporting phase shown in Fig. 2, the zero-velocity detection algorithm can be used to determine whether the foot is in the standing middle phase. Among them, the amplitude detection method is the most basic method [33–36]. In theory, when the foot velocity is zero, the amplitude of the accelerometer measurement is the amplitude of the local gravity acceleration, and the angular velocity of the gyroscope should be zero. The core judgment formula of zero velocity detection based on this principle is

$$\begin{cases} \xi(Z_k^a) = \frac{1}{\sigma_a^2 W}\sum_{l=k}^{k-W+1}\left(\|\boldsymbol{f}_l^b\| - \|\boldsymbol{g}\|\right)^2 \\ \xi(Z_k^w) = \frac{1}{\sigma_\omega^2 W}\sum_{l=k}^{k+W-1}\|\boldsymbol{\omega}_l\|^2 \end{cases} \quad (2)$$

where, $||\cdot||$ is modulus; $\boldsymbol{g}$ is local gravity acceleration; σ_a^2, σ_ω^2 are the ratio of the square of the accelerometers and gyroscopes modulus to the variance of the self-noise respectively. W is the length of the detection window.

The calculation results of Eq. (2) should be compared with the thresholds instead of comparing with zero directly due to the measurement noise. When the results are less than the thresholds, the current time is judged to be zero velocity state; otherwise, the current time is judged to be non-zero velocity state. The threshold is obtained by processing the data in the static state which need many tests.

2.2.3. Basic ZUPT algorithm

The theoretical velocity should be zero when the pedestrian gait is detected as stationary, that is the velocity component of the foot MIMU navigation solution should be zero. However, due to MIMU noise, the actual velocity is not zero but the pedestrian's velocity error. Using velocity error as the observation, the Kalman filter can be used to estimate and correct the navigation error. Based on this principle, the system state equation and the measurement equation are established as

$$\begin{aligned} \dot{\boldsymbol{X}} &= \boldsymbol{A}\boldsymbol{X} + \boldsymbol{\eta_k} \\ \boldsymbol{Z} &= \boldsymbol{H}\boldsymbol{X} + \boldsymbol{v_k} \end{aligned} \tag{3}$$

where, $\boldsymbol{X} = \begin{bmatrix} \delta\boldsymbol{p}^T & \delta\boldsymbol{v}^T & \boldsymbol{\Phi}^T & \boldsymbol{\Delta}^T & \boldsymbol{\varepsilon}^T \end{bmatrix}^T$ is the state of the system, $\delta\boldsymbol{p}$, $\delta\boldsymbol{v}$, $\boldsymbol{\Phi}$ are position error, velocity error, and misalignment angle respectively; $\boldsymbol{\Delta}$, $\boldsymbol{\varepsilon}$ are accelerometer bias and gyro drift respectively; $\boldsymbol{H} = [\boldsymbol{O}_{3\times3} \quad \boldsymbol{I}_{3\times3} \quad \boldsymbol{O}_{3\times3} \quad \boldsymbol{O}_{3\times3} \quad \boldsymbol{O}_{3\times3}]$ is the measure matrix; $\boldsymbol{Z}$ is the observation; $\boldsymbol{\eta_k}$, $\boldsymbol{v_k}$ are state noise and measurement noise respectively; $\boldsymbol{A}$ is the system transfer matrix and the specific form is

$$\boldsymbol{A} = \begin{bmatrix} \boldsymbol{O}_{3\times3} & \boldsymbol{I}_{3\times3} & \boldsymbol{O}_{3\times3} & \boldsymbol{O}_{3\times3} & \boldsymbol{O}_{3\times3} \\ \boldsymbol{O}_{3\times3} & \boldsymbol{O}_{3\times3} & \left[\tilde{\boldsymbol{f}^n}\times\right] & \boldsymbol{C}_b^n & \boldsymbol{O}_{3\times3} \\ \boldsymbol{O}_{3\times3} & \boldsymbol{O}_{3\times3} & \boldsymbol{O}_{3\times3} & \boldsymbol{O}_{3\times3} & -\boldsymbol{C}_b^n \\ \boldsymbol{O}_{3\times3} & \boldsymbol{O}_{3\times3} & \boldsymbol{O}_{3\times3} & \boldsymbol{O}_{3\times3} & \boldsymbol{O}_{3\times3} \\ \boldsymbol{O}_{3\times3} & \boldsymbol{O}_{3\times3} & \boldsymbol{O}_{3\times3} & \boldsymbol{O}_{3\times3} & \boldsymbol{O}_{3\times3} \end{bmatrix}$$

However, a conclusion can be obtained by linearity system observability analysis for ZUPT: the velocity error and the horizontal misalignment angle can be observed, the positioning error and the azimuth misalignment angle are unobservable [39,40]. This is the disadvantage and deficiency of the ZUPT algorithm for foot-mounted initial position system.

3. Dual-foot positioning algorithm based on adaptive inequality constraints Kalman filter (AICKF)

According to the character 4 in Section 2.1, the relative distance between the two feet is approximately constant when one foot is in the standing initial phase and the other foot is in the standing ending phase. The distance between the two feet changes in real time when one foot is in the standing middle phase, the other foot is in the swing phase. Combined with this conclusion, the process of the relative distance between two feet in a gait is shown in the Fig. 4.

Here, $\boldsymbol{D}_j$ $(j = K, \cdots, K+N)$ is the distance between two feet at the time j; At moment K, the left foot is in the standing initial phase, and the right foot is in the standing ending phase; At moment $K+N$, the left foot is in the standing ending phase, ready to enter the swing phase, and the right foot is in the standing initial phase. Therefore, at moment K and $K+N$, both feet are in the standing phase.

One characteristic of pedestrian gait is symmetry. According to the symmetry of step size, $\boldsymbol{D}_K \approx \boldsymbol{D}_{K+N}$, that is $\boldsymbol{D}_K/\boldsymbol{D}_{K+N} \approx 1$. In general, the deviation is within ±0.05. In addition, when $K < k < K+N$, there is $\boldsymbol{D}_k \le \boldsymbol{D}_K$. Therefore, the constraint of the relative position of the two feet is established during the pedestrian walking.

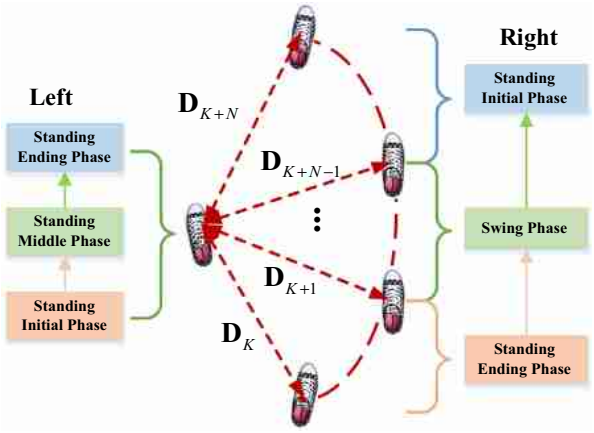

Fig. 4. Relative distance between two feet in one gait.

$$\boldsymbol{B}\boldsymbol{x}_k \le \boldsymbol{D}_k \tag{4}$$

where, k is the sample time; $\boldsymbol{B} = [\boldsymbol{I}_{3\times3} \quad \boldsymbol{O}_{3\times12} \quad -\boldsymbol{I}_{3\times3} \quad \boldsymbol{O}_{3\times12}]$, $\boldsymbol{x} = \begin{bmatrix} \boldsymbol{x}_L^T & \boldsymbol{x}_R^T \end{bmatrix}^T$, $\boldsymbol{x}_L^T = \begin{bmatrix} \delta\boldsymbol{p}_L^T & \delta\boldsymbol{v}_L^T & \boldsymbol{\Phi}_L^T & \boldsymbol{\Delta}_L^T & \boldsymbol{\varepsilon}_L^T \end{bmatrix}^T$, $\boldsymbol{x}_R^T = \begin{bmatrix} \delta\boldsymbol{p}_R^T & \delta\boldsymbol{v}_R^T & \boldsymbol{\Phi}_R^T & \boldsymbol{\Delta}_R^T & \boldsymbol{\varepsilon}_R^T \end{bmatrix}^T$. R, L are the right and left foot respectively; $\boldsymbol{D}_k$ is the constraint parameter of two feet.

The meaning of $\boldsymbol{D}_k$ is the distance between two feet. Hence, it can be obtained by calculating the difference between the two feet position information. And the value of $\boldsymbol{D}_k$ is different for every gait. Therefore, $\boldsymbol{D}_k$ is adjusted adaptively with each gait, and the adjustment method is as follows,

$$\boldsymbol{D}_k = \begin{cases} \tilde{\boldsymbol{p}}_{Lk}^n - \tilde{\boldsymbol{p}}_{Rk}^n & F_{LSP} \times F_{RSEP} = 1 \quad or \quad F_{RSP} \times F_{LSEP} = 1 \\ \boldsymbol{D}_{k-1} & else \end{cases} \tag{5}$$

where, $\tilde{\boldsymbol{p}}_{Lk}^n$ and $\tilde{\boldsymbol{p}}_{Rk}^n$ are the position result of the left and right foot by Eq. (1) respectively; F_{LSP} and F_{RSP} are the flags indicating that the left foot and the right foot are in the standing initial phase respectively. If the value is 1, indicating it is in this phase. If the value is 0, indicating it is not in this phase; F_{LSEP} and F_{RSEP} are the flags indicating that the left foot and the right foot are in the standing ending phase. If the value is 1, indicating it is in this phase. If the value is 0, indicating it is not in this phase.

The state quantity constraint for the ZUPT is introduced by Eq. (4), and the constraint is used for constraint the position error. Thus, ZUPT based on inequality constrained Kalman filter can be used to correct part of navigation error. The problem can be solved by the local minimum point of quadratic programming and the maximum likelihood method [37,38], as shown by (6).

$$\begin{aligned} &\min_x (\tilde{\boldsymbol{x}}^T \boldsymbol{P}^{-1} \tilde{\boldsymbol{x}} - 2\hat{\boldsymbol{x}}^T \boldsymbol{P}^{-1} \tilde{\boldsymbol{x}}) \\ &\boldsymbol{B}\tilde{\boldsymbol{x}}_k \le \boldsymbol{D}_k \end{aligned} \tag{6}$$

where, $\hat{\boldsymbol{x}}$ is the estimation result of unconstrained Kalman filter state quantity; $\boldsymbol{P}$ is the unconstrained Kalman filter covariance matrix; $\tilde{\boldsymbol{x}}$ is the estimation result of constrained Kalman filter state quantity.

In addition, the precondition of introducing the unconstrained Kalman filter to the ZUPT is pedestrian gait is symmetry. However, the symmetry is satisfied when the pedestrian is walking straight. For example, the symmetry is not satisfied when the pedestrian

turning around. Therefore, the z-axis (up) angular velocity of the foot measured by gyros is used to judge the state of walking. If the value of the z-axis angular velocity is smaller than the threshold, the unconstrained equation works for Kalman Filter. If the value of the z-axis angular velocity is bigger than the threshold, the unconstrained equation cannot be used.

4. Pedestrian positioning optimization algorithm based on dynamic magnetic disturbance compensation (DMDC)

Magnetometer is a sensor that measures the local projection of earth's magnetic field. When the magnetometer and MIMU are installed to the feet of the pedestrian, the projection of the local magnetic field strength along the installation coordinate system can be measured in real time. Then according to the basic principle of magnetic field intensity projection, the orientation information can be calculated.

However, since the magnetometer is susceptible to ambient magnetic interference, there is an error in measurement azimuth. The magnetometer measurement model is established as follows

$$\boldsymbol{y}_m^b = \boldsymbol{C}_n^b \boldsymbol{m}^n + \boldsymbol{h} + \upsilon \tag{7}$$

where, $\boldsymbol{y}_m^b$ is the measurement output of the magnetometer along the b frame; $\boldsymbol{m}^n = \begin{bmatrix} \cos\alpha & 0 & \sin\alpha \end{bmatrix}^T$ is the projection result of the constant value along the n-coordinate frame, α is the magnetic inclination, which is related to the geographical latitude, and can be obtained by lookup; $\boldsymbol{h}$ is the projection value of the magnetic constant interference, which is produced by the sensor itself and not changed in different environment; υ is the magnetic measurement noise, including the magnetic interference produced by the application environment, and it will be changed in real time. For example, magnetic interference can be produced by the electrical wire along the walk side.

According to the conversion relationship of the strapdown matrix $\boldsymbol{C}_{\tilde{n}}^b = \boldsymbol{C}_n^b \boldsymbol{C}_{\tilde{n}}^n$, $\boldsymbol{C}_{\tilde{n}}^n = \boldsymbol{I} + [\Phi\times]$, the Eq. (7) can be adjusted to

$$\boldsymbol{y}_m^b - \boldsymbol{C}_n^b \boldsymbol{m}^n = \boldsymbol{C}_n^b [\boldsymbol{m}^n\times]\Phi + \boldsymbol{h} + \upsilon \tag{8}$$

where, $\Phi = \begin{bmatrix} \phi_x & \phi_x & \phi_x \end{bmatrix}^T$ is the triaxial misalignment angle; $[\cdot\times](\cdot = \Phi, \boldsymbol{m}^n)$ is the antisymmetric matrix of the vector $\cdot$.

Combining Eqs. (3) and (8), the state equation and measurement equation of dynamic magnetic interference can be established

$$\begin{aligned} \dot{\boldsymbol{x}}_m &= \boldsymbol{A}_m \boldsymbol{x}_m + \boldsymbol{\eta}_m \\ \boldsymbol{z}_m &= \boldsymbol{H}_m \boldsymbol{x}_m + \upsilon \end{aligned} \tag{9}$$

where, $\boldsymbol{x}_m$ is the state of the system, and the form is,

$$\boldsymbol{x}_m = \begin{bmatrix} \Phi^T & \varepsilon^T & \boldsymbol{h}^T \end{bmatrix}^T$$

$\boldsymbol{A}$ is the system transfer matrix, and the form is,

$$\boldsymbol{A} = \begin{bmatrix} \boldsymbol{O}_{3\times3} & -\boldsymbol{C}_b^n & \boldsymbol{O}_{3\times3} \\ \boldsymbol{O}_{3\times3} & \boldsymbol{O}_{3\times3} & \boldsymbol{O}_{3\times3} \\ \boldsymbol{O}_{3\times3} & \boldsymbol{O}_{3\times3} & \boldsymbol{O}_{3\times3} \end{bmatrix}$$

$\boldsymbol{z}_m$ is the observation, and the form is,

$$\boldsymbol{z}_m = \boldsymbol{y}_m^b - \boldsymbol{C}_n^b \boldsymbol{m}^n$$

$\boldsymbol{H}_m$ is the measure matrix, the form is,

$$\boldsymbol{H}_m = \begin{bmatrix} \boldsymbol{C}_n^b [\boldsymbol{m}^n\times] & \boldsymbol{O}_{3\times3} & \boldsymbol{I}_{3\times3} \end{bmatrix}$$

where, ε, $\boldsymbol{h}$ are gyro drift and magnetic constant interference respectively; $\boldsymbol{\eta}_m$, υ are state noise and measurement noise respectively; $\boldsymbol{C}_{\tilde{n}}^b$ is calculated by dead reckoning by Eq. (1); $\boldsymbol{I}_{3\times3}$ is a unit array.

It can be obtained that the system described in (9) is a linear time-varying system. According to the observability of the linear time-varying system given in the literature [21], the magnetometer constant interference $\boldsymbol{h}$ can be calibrated by Kalman Filter when the calibration environment includes static environment and dynamic environment containing triaxial angular motion. During the walking process, when foot is in the standing phase, the magnetometer is in a stationary state; when foot is in the swing phase, the three axes of the magnetometer include angular motion. Combining Eq. (9) with Kalman filter, the magnetic interference can be estimated under the pedestrian walking, and the accuracy of the heading angle estimated by the magnetometer measurement value can be improved after compensation.

However, the precondition of using Kalman Filter to estimate $\boldsymbol{h}$ is the statistical property of the measurement noise is known. According to Eq. (7) and the definition of the parameter of υ, it can be obtained that the statistical property of υ will be changed with the magnetic interference in different application environment. Therefore, an adaptive parameter is introduced in the Kalman Filter to avoid the influence of the changing magnetic interference on the pedestrian position.

There are two parameters of Kalman Filter reflect the changing magnetic interference: One is the observation $\boldsymbol{z}_m$ of Kalman Filter. The value of $\boldsymbol{y}_m^b$ will be changed if the changing magnetic interference increase, then the value of $\boldsymbol{z}_m$ will changes; The other parameter reflects the changing magnetic interference in Kalman Filter is the covariance matrix $\boldsymbol{P}$. $\boldsymbol{P}$ will be changed by many factors, such as unknown bias, inaccuracy model, magnetic interference and so. Hence, the observation $\boldsymbol{z}_m$ and the covariance matrix $\boldsymbol{P}$ are introduced to calculating the adaptive parameter for updating the statistical property of the measurement noise, which reflect the observation changing caused by the changing magnetic interference. The calculating method for the adaptive parameter is

$$\begin{aligned} \boldsymbol{\beta}_1 &= \tfrac{1}{M-1} \sum_{j=k-M+1}^{k} (\boldsymbol{z}_{mj} - \boldsymbol{H}_{mj}\boldsymbol{x}_{mj})(\boldsymbol{z}_{mj} - \boldsymbol{H}_{mj}\boldsymbol{x}_{mj})^T \\ \boldsymbol{\beta}_2 &= (\boldsymbol{z}_{mk} - \boldsymbol{H}_{mk}\boldsymbol{x}_{mk})(\boldsymbol{z}_{mk} - \boldsymbol{H}_{mk}\boldsymbol{x}_{mk})^T \\ \boldsymbol{\beta}_3 &= \boldsymbol{H}_{mk}\boldsymbol{P}_k^- \boldsymbol{H}_{mk}^T + \boldsymbol{R}_k \\ \boldsymbol{\beta} &= \tfrac{1}{2} \cdot |tr\boldsymbol{\beta}_2 + tr\boldsymbol{\beta}_3 - 2 \cdot tr\boldsymbol{\beta}_1| \end{aligned} \tag{10}$$

where, M is the time period; tr is the trace of a matrix; $\boldsymbol{R}_k$ is observation noise variance, which is set at the beginning.

According to Eq. (10), it can be seen that, $\boldsymbol{\beta}_1$ is the mean of difference between the observation $\boldsymbol{z}_{mj}$ and the observation forecasting $\boldsymbol{H}_{mj}\boldsymbol{x}_{mj}$ during time period of $M-1$. $\boldsymbol{\beta}_2$ is the difference between the observation $\boldsymbol{z}_{mk}$ and the observation forecasting $\boldsymbol{H}_{mk}\boldsymbol{x}_{mk}$ at time k. $\boldsymbol{\beta}_3$ is the covariance matrix of the observation. Therefore, if the magnetic interference stable, the value of $\boldsymbol{\beta}$ close to zero. If the magnetic interference changed at time k, the observation noise variance set at the beginning is not suitable for time k. And the value of $\boldsymbol{\beta}_2$ and $\boldsymbol{\beta}_3$ all increases, and the value of $\boldsymbol{\beta}$ also increases. Hence, $\boldsymbol{\beta}$ can reflects the changing magnetic interference in real time. Then, the Kalman Filter is changed by introducing the adaptive parameter $\boldsymbol{\beta}$.

$$\begin{aligned} \hat{\boldsymbol{x}}_{nk}^- &= \Phi_k \hat{\boldsymbol{x}}_{m(k-1)} \\ \boldsymbol{P}_k^- &= \Phi_k \boldsymbol{P}_{k-1} \Phi_k^T + \boldsymbol{Q}_k \\ \boldsymbol{K}_k &= \boldsymbol{P}_k^- \boldsymbol{H}_{mk}^T (\boldsymbol{H}_{mk} \boldsymbol{P}_k \boldsymbol{H}_{mk}^T + \beta \boldsymbol{R}_k)^{-1} \\ \hat{\boldsymbol{x}}_{mk} &= \hat{\boldsymbol{x}}_{mk}^- + \boldsymbol{K}_k (\boldsymbol{Z}_{mk} - \boldsymbol{H}_{mk} \hat{\boldsymbol{x}}_{mk}^-) \\ \boldsymbol{P}_k &= (\boldsymbol{I} - \boldsymbol{K}_k \boldsymbol{H}_{mk}) \boldsymbol{P}_k^- \end{aligned} \tag{11}$$

The adaptive parameter β is introduced to updating the statistical property of the measurement noise. Then the attitude, which is obtained by the magnetometer without magnetic interference, is used as the ZUPT observation to decrease the position error of the pedestrian position. However, the magnetic interference is much larger than the earth magnetic field sometimes, and the magnetic error cannot be estimated by Kalman Filter. Hence, the first step of using the magnetometer as the external sensor for the inertial pedestrian position system is judging whether the magnetic interference within the limits.

Only magnetic field can be measured by the magnetometers without ant magnetic interference, and the measurement value nearly constant in a small field. The magnetic field can be lookup if the latitude is known. Therefore, the magnetic error, which is the difference between the magnetometer's measurement and the magnetic field in theory, can be used to judge the strength of the magnetic interference.

$$\sigma = \left| \|\boldsymbol{y}^b\| - \|\boldsymbol{m}^n\| \right| \tag{12}$$

where, $\|\cdot\|$ is the module value of vector $\cdot$.

5. Scheme of improved pedestrian position algorithm and performance evaluation

5.1. Scheme of improved pedestrian position algorithm

According to the basic pedestrian positioning method in Section 2, the positioning and orientation information optimization algorithm in Section 3 and 4, Fig. 5 shows a schematic diagram of the improved pedestrian positioning.

In the figure, the green part is the inherent solution unit of the traditional pedestrian positioning method, including dead reckoning, ZVD; the red part is the newly added or improving unit, including the dual-foot MIMU data acquisition, ZUPT based on AICKF, and optimized azimuth solving unit based on dynamic magnetic interference compensation. Therefore, the steps of the pedestrian positioning method proposed in this paper are as follows:

(1) Collect dual foot-mounted MIMU measurement data (acceleration, angular velocity, magnetic);
(2) Navigation information solution based on dead reckoning method (Eq. (1));
(3) Dual-foot azimuth angle solution based on dynamic magnetic interference compensation (Eqs. (9)–(12));
(4) Gait state judgment, if the feet are in the standing phase, calculate the inequality constraints condition (Eq. (6));
(5) When the foot touches the ground, the ZUPT based on AICKF is calculated by using the constraints of step 3 and step 4. Then estimate and compensate the navigation error, and obtain the pedestrian positioning result. The system state equation and ZUPT equation for the estimation process are as follows,

$$\begin{aligned} \dot{\boldsymbol{x}} &= \boldsymbol{A}\boldsymbol{x} + \boldsymbol{\eta}_k \\ \boldsymbol{z} &= \boldsymbol{H}\boldsymbol{x} + \boldsymbol{v}_k \\ \boldsymbol{B}\boldsymbol{x} &\le \boldsymbol{D} \end{aligned} \tag{13}$$

where, $\boldsymbol{x} = \left[\boldsymbol{x}_L^T \quad \boldsymbol{x}_R^T\right]^T$, $\boldsymbol{x}_L^T = \left[\delta\boldsymbol{p}_L^T \quad \delta\boldsymbol{v}_L^T \quad \boldsymbol{\Phi}_L^T \quad \boldsymbol{\Delta}_L^T \quad \boldsymbol{\varepsilon}_L^T\right]^T$, $\boldsymbol{x}_R^T = \left[\delta\boldsymbol{p}_R^T \quad \delta\boldsymbol{v}_R^T \quad \boldsymbol{\Phi}_R^T \quad \boldsymbol{\Delta}_R^T \quad \boldsymbol{\varepsilon}_R^T\right]^T$;

The state matrix is as follow,

$$\boldsymbol{A} = \begin{bmatrix} \boldsymbol{A}_L & \boldsymbol{O}_{15\times15} \\ \boldsymbol{O}_{15\times15} & \boldsymbol{A}_R \end{bmatrix}$$

where, $\boldsymbol{A}_L$,$\boldsymbol{A}_R$ are the conversion matrix of the left foot and the right foot respectively, the form is the same as the Eq. (3); the measurement matrix $\boldsymbol{H}$ should be switched as the state of the feet change, according to the following

$$\boldsymbol{H} = \begin{cases} [\boldsymbol{O}_{3\times3} \quad \boldsymbol{I}_{3\times3} \quad \boldsymbol{I}_{3\times3} \quad \boldsymbol{O}_{3\times3} \quad \boldsymbol{O}_{3\times3} \quad \boldsymbol{O}_{3\times15}] & \textit{if left foot in the standing middle phase} \\ [\boldsymbol{O}_{3\times15} \quad \boldsymbol{O}_{3\times3} \quad \boldsymbol{I}_{3\times3} \quad \boldsymbol{I}_{3\times3} \quad \boldsymbol{O}_{3\times3} \quad \boldsymbol{O}_{3\times3}] & \textit{if right foot in the standing middle phase} \end{cases}$$

5.2. Performance evaluation

To verify the improved pedestrian positioning algorithm, MTi-G710 inertial sensor (includes gyroscopes, accelerometers and magnetometers) produced by XSENS company is used to build a test equipment. During the experiment, two MTi-G710 MIMUs were installed on two feet. The STM32 MCU collects MIMU measurement data in real time, including angular velocity, acceleration, and magnetometer measurements. The test equipment is shown in Fig. 6. The unit of angular velocity is rad/s, and the acceleration unit is m/s^2, and the magnetometer measurement value is normalized.

In addition, the threshold, which is mentioned in the last paragraph of section 3 and used to judge whether pedestrian is walking straight, is set with 6 rad/s. The output of the MTi-G710 magnetometer is in arbitrary units (a.u.). Whereas one a.u. is the magnetic field strength during calibration at XSENS calibration lab. Hence, the parameter σ in Eq. (12) is set 1, which means that the DCDM will not work if the magnetic interference is twice as much as the magnetic field.

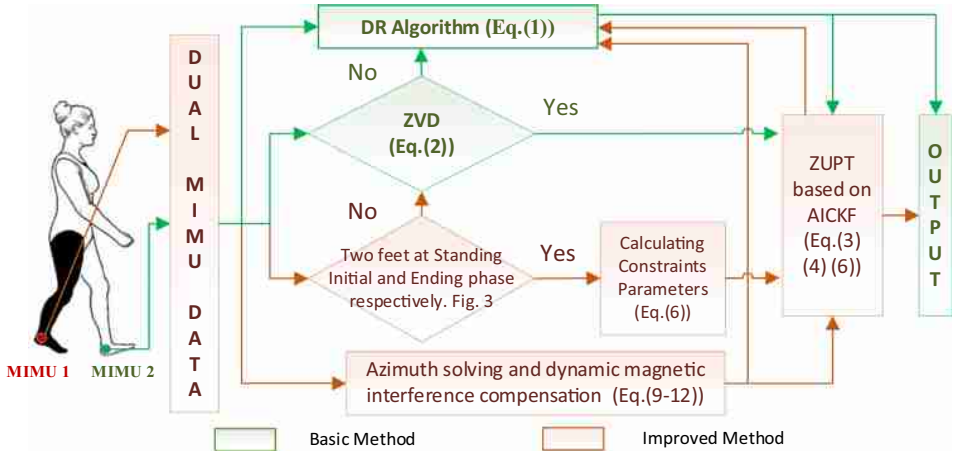

Fig. 5. Dual Foot-Mounted Inertial/Magnetometer Pedestrian Positioning Based on AICKF.

Fig. 6. The position and the orientation of externally located MTi-G710 on Shoe.

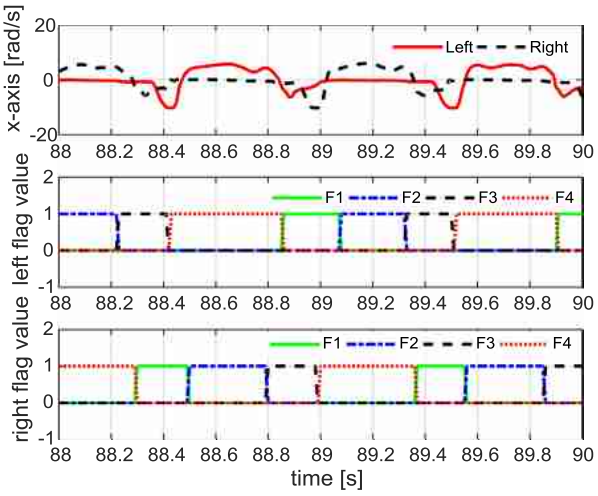

Fig. 7. Judgment results of different states in one gait.

Fig. 7 is the foot phase for one gait. The signs and its value meanings of different stages are shown in Table 2. Combining the definition of Table 2 with the experimental results of Fig. 7, the result is consistent with the analysis of pedestrian gait characteristics in Section 2.1. The angular velocity measured by the x-axis gyroscope can effectively judge the instant of the heel touchdown and the toe leaves the ground, further the gait is divided into swing phase and standing phase. Based on the conclusion above, the ZUPT method can effectively distinguish the standing initial phase, standing middle phase and standing ending phase. In addition, comparing the judgment results of the two feet, when one foot is in the standing initial phase and the other foot is in the standing ending phase, the inequality constrains condition can be calculated by using this stage.

Two groups of walking experiments were carried out, and the relevant parameters are shown in Table 3. The magnetometer estimation result is shown in the Fig. 8(a) and (c) are magnetic interference estimation results, and (b) and (d) are magnetic field strength measurement results before and after magnetic interference compensation. Fig. 9 shows the results of two groups of dual foot positioning curve of basic method and the improved method in this paper. In addition, the curves in Fig. 9 are obtained by different methods, the illustration of the legend is shown as follows:

- Right-ZUPT with KF: the right foot of pedestrian position information calculated by basic ZUPT algorithm, and it is described in section 2.2.1;
- Right- ZUPT with KF + DMDC: the right foot of pedestrian position information calculated by basic ZUPT algorithm (section 2.2.1) and the Dynamic Magnetic Disturbance Compensation algorithm described in section 4;
- Right- ZUPT with AICKF + DMDC: the right foot of pedestrian position information calculated by improved ZUPT algorithm of AICKF (section 3) and the Dynamic Magnetic Disturbance Compensation algorithm described in section 4;
- Left – ZUPT with KF: the left foot of pedestrian position information calculated by basic ZUPT algorithm, and it is described in section 2.2.1;
- Left – ZUPT with KF + DMDC: the left foot of pedestrian position information calculated by basic ZUPT algorithm (section 2.2.1) and the Dynamic Magnetic Disturbance Compensation algorithm described in section 4;
- Left – ZUPT with AICKF + DMDC: the left foot of pedestrian position information calculated by improved ZUPT algorithm of AICKF (section 3) and the Dynamic Magnetic Disturbance Compensation algorithm described in section 4;
- Start Point: the start points of the trajectory in the experiment.

It can be seen from the magnetic interference estimation results in Fig. 8 that the estimation results of the same coordinate axes of the two feet are close. Because the two feet are in the same magnetic interference environment during the walking process. However, the three-axis magnetic interference estimation results do not tend to be stable, because as the pedestrian walks, the surrounding environment changes, and the magnetic interference also changes. So, the three axes are subject to different levels of magnetic interference. It can be seen from the Fig. 8(b) that before the magnetic interference compensation, the magnetic field strength measurement result is unstable and there is a slow drift. It corresponds to the analysis result of figure (a), that is, the magnetic interference change affects the magnetic measurement

Table 2
Flags and Their meanings in Fig. 7.

No.	Stage	Flag	The meaning of "1"	The meaning of "0"
1	Standing initial phase	F1	At this stage	Not at this stage
2	Standing middle phase	F2	At this stage	Not at this stage
3	Standing ending phase	F3	At this stage	Not at this stage
4	Swing phase	F4	At this stage	Not at this stage

Table 3
The relevant parameters of experiments.

No.	Experiment	Trajectory	Length(m)	Time(s)	Sampling frequency (Hz)
1	Test 1	Straight	87.2	100	100 Hz
2	Test 2	L-shaped	120	130	100 Hz

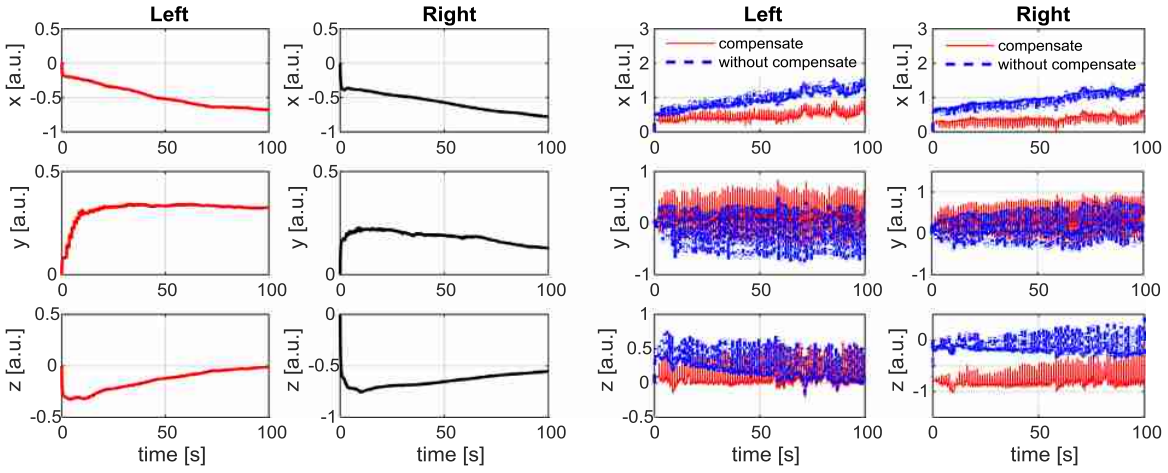

(a)Magnetic interference estimation of test 1

(b) Magnetic field intensity before and after compensation of test 1

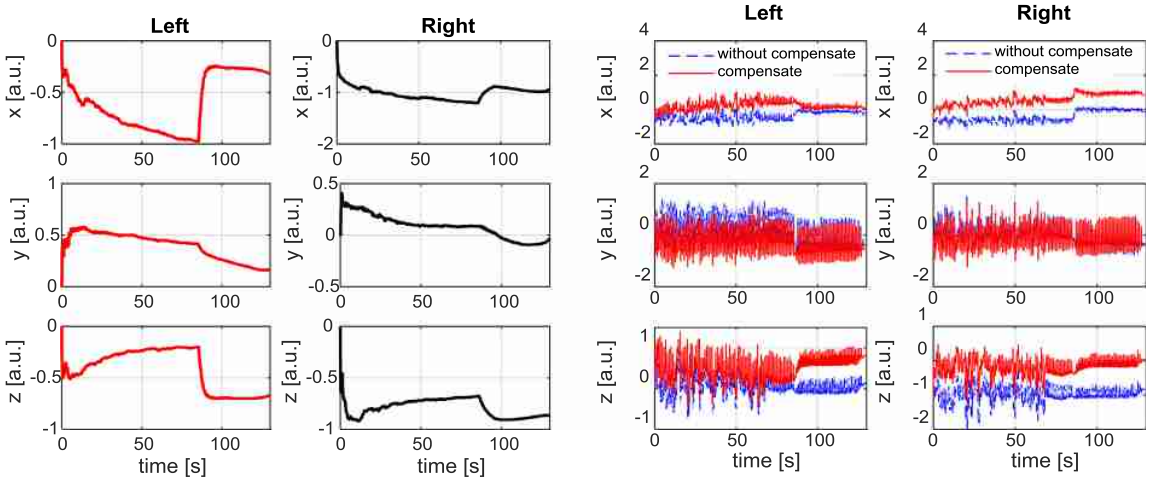

(c)Magnetic interference estimation of test 2

(d) Magnetic field intensity before and after compensation of test 2

Fig. 8. Magnetometer experimental results.

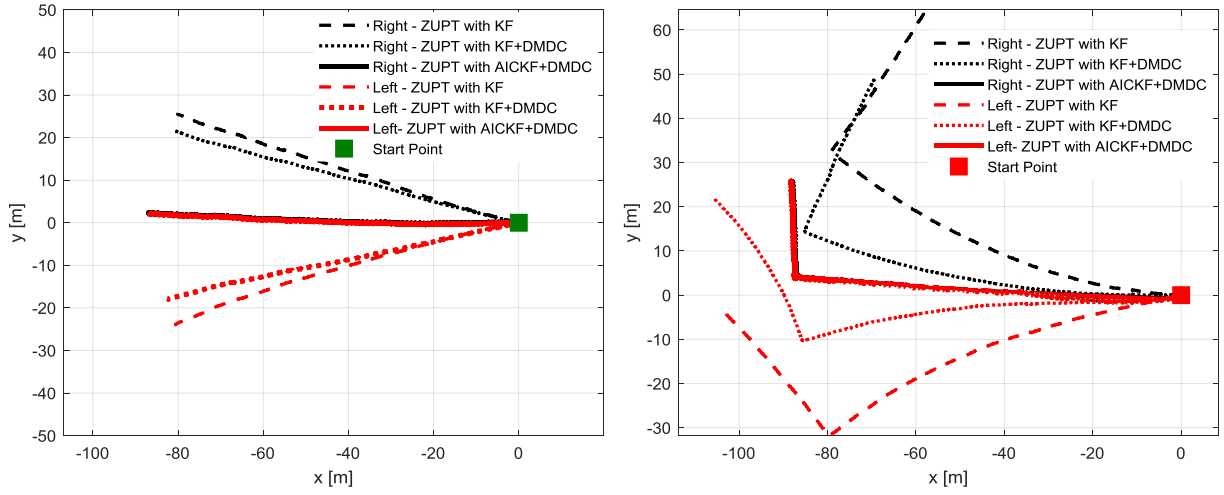

(a) Test 1

(b) Test 2

Fig. 9. Dual foot positioning curve of basic algorithm and improved algorithm.

results. However, the measurement of the magnetic field strength before and after the magnetic interference compensation is stable, which is consistent with the conclusion that the earth's magnetic field projection is nearly constant along the local coordinate system.

Compared the position result obtained by the "ZUPT with KF" algorithm with that obtained by the "ZUPT with KF + DCDM" algorithm, it can be seen that, the position error is decreased by estimating and compensating the magnetic interference. Compared the position result obtained by the "ZUPT with AICKF + DCDM" algorithm with that obtained by the other two algorithms, it can be seen that, the azimuth misalignment angle can be estimated and corrected by the magnetometer azimuth and the AICKF algorithm. In addition, introducing inequality constraint in the Kalman filter can effectively reduce the positioning error, especially as the walking time becomes longer, the cumulative positioning error of the traditional ZUPT method becomes larger. For Test 1, the positioning error of the two feet is corrected from 25 m to 2 m; for Test 2, the positioning error of the two feet is corrected to 3 m. Although the AICKF method cannot guarantee the stability of long-term positioning accuracy, such as walking time longer than 10 min, but when walking time is about 100 s, compared with the traditional ZUPT method, AICKF effectively improves the accuracy of pedestrian walking positioning based on inertial sensors.

6. Conclusion

For the inertial foot-mounted pedestrian positioning system, the basic ZUPT algorithm cannot correct the positioning error and the azimuth misalignment angle, which leads to the problem that the positioning error increases with the time. Based on the analysis of pedestrian gait motion characteristics, a dual foot-mounted positioning algorithm based on adaptive inequality constraints Kalman filter is proposed. When one foot is in the standing initial phase and the other foot is in the standing ending phase, the relative distance between the two feet is approximately constant. With this characteristic, the adaptive adjustment inequality constraint is introduced to Kalman filter of ZUPT. For the problem that the azimuth misalignment angle cannot be observed, a walking azimuth optimization algorithm based on dynamic magnetic interference compensation is proposed. When the characteristics of pedestrian motion meets the condition of dynamic magnetic interference observation, the magnetic interference is estimated and compensated in real time. And then, the azimuth is provided as the observation to improve the system observability, correct the system navigation error and improve positioning accuracy. Finally, MTi-G710 sensor produced by XSENS is used to carry out the experiment. The test includes two paths, linear and L-shaped. The validity and applicability of the proposed method are validated through the result curves of the magnetic interference estimation and the trajectory tracking.

Acknowledgement

The paper is supported by National Natural Science Foundation of China (No. 51509049, 51879046), Special Funds for Scientific and Technological Innovation of Harbin (No. 2016RAQXJ022).

References

[1] Dailin Li, Yanlei Gu, Shusuke Kamijo. Pedestrian positioning in urban environment by integration of PDR and traffic mode detection, in: 2017 IEEE 20th International Conference on Intelligent Transportation Systems. Yokohama, Japan. October 2017.
[2] Gu Yang, Caifa Zhou, Andreas Wieser, Zhimin Zhou, Pedestrian Positioning Using WiFi Fingerprints and a Foot-mounted Inertial Sensor, European Navigation Conference, Lausanne, 2017.
[3] Alejandro Correa, Estefania Munoz Diaz, Dina Bousdar Ahmed, Advanced pedestrian positioning system to smartphones and smartwatches, Sensors 16 (11) (2016).
[4] Anahid Basiri, Pouria Amirian, Adam Winstanley, Stuart Marsh, Seamless pedestrian positioning and navigation using landmarks, J. Navig. 69 (1) (2016) 24–40.
[5] R. Harle, A survey of indoor inertial positioning systems for pedestrians, IEEE Commun. Surv. Tutor. 99 (2013) 1–13.
[6] Carl Fischer, Poorna Talkad Sukumar, Mike Hazas, Tutorial: implementing a Pedestrian Tracker Using Inertial Sensors, IEEE Pervasive Comput. 12 (2) (2013) 17–27.
[7] J. Elwell, Inertial Navigation for the Urban Warrior, Proc. of Digitization of the Battlespace IV, SPIE. 3709 (1999) 196–204.
[8] L. Ojeda, J. Borenstein, Non-GPS navigation for security personnel and first responders, J. Navig. 60 (3) (2007) 391–407.
[9] E. Foxlin, Pedestrian tracking with shoe-mounted inertial sensors, IEEE Comput. Graphics Appl. 25 (6) (2005) 38–46.
[10] Ö. Bebek et al., Personal navigation via high-resolution gait corrected inertial measurement units, IEEE Trans. Instrum. Meas. 59 (11) (2010) 3018–3027.
[11] J.O. Nilsson, I. Skog, P. Händel, Khari, in: Foot-mounted inertial navigation for everybody-an open-source embedded implementation. IEEE/ION Position, Location and Navigation Symposium (PLANS), Myrtle Beach, SC, USA, 2012, pp. 23–26.
[12] Qiuying Wang, Zheng Guo, Zhiguo Sun, Xufei Cui, Kaiyue Liu, Research on the forward and reverse calculation based on the adaptive zero-velocity interval adjustment for the foot-mounted inertial pedestrian-positioning, System. Sensors. 18 (5) (2018).
[13] S. Godha, G. Lachapelle, Foot mounted inertial system for pedestrian navigation, Meas. Sci. Technol. 19 (2008) 1–9.
[14] H.M. Schepers, H.F.J.M. Koopman, P.H. Veltink, Ambulatory assessment of ankle and foot dynamics, IEEE Trans. Biomed. Eng. 54 (5) (2007) 895–902.
[15] D.O. King, K.M. Brunson, MEMS Self-Resonant Magnetometer, WO2005029107-A1, 2005.
[16] W. Zhang, M. Guang, H.-G. Li, Modeling and simulation of the squeeze film effect on the MEMS structures, in: 2005 Asia-Pacific Microwave Conference Proceedings, Suzhou, China, 2005; Vol. 2, pp. 1–3.
[17] Dahai Ren, Wu. Lingqi, Meizhi Yan, Mingyang Cui, Zheng You, Hu. Muzhi, Design and analyses of a MEMS based resonant magnetometer, Sensors 9 (2009) 6951–6966.
[18] Manon Kok, Thomas B. Schön, Magnetometer calibration using inertial sensors, IEEE Sens. J. 16 (14) (2016) 5679–5690.
[19] J. Metge, R. Mégret, A. Giremus, Y. Berthoumieu, T. Décamps, Calibration of an inertial-magnetic measurement unit without external equipment, in the presence of dynamic magnetic disturbances, Meas. Sci. Technol. 25 (12) (2014) 106–125.
[20] J.F. Vasconcelos, G. Elkaim, C. Silvestre, P. Oliveira, B. Cardeira, Geometric approach to strapdown magnetometer calibration in sensor frame, IEEE Trans. Aerosp. Electron. Syst. 47 (2) (2011) 1293–1306.
[21] Wu. Yuanxin, Danping Zou, Peilin Liu, Yu. Wenxian, Dynamic magnetometer calibration and alignment to inertial sensors by Kalman Filtering, IEEE Trans. Control Syst. Technol. 26 (2) (2018) 716–723.
[22] Jiménez Antonio, Seco Fernando, J. Carlos Prieto Honorato, I. Guevara Rosas, Jorge. Pedestrian indoor navigation by aiding a foot-mounted IMU with RFID Signal Strength measurements. 2010 International Conference on Indoor Positioning and Indoor Navigation, IPIN 2010 – Conference Proceedings. 1 – 7.
[23] Antonio Ramón Jimenez Ruiz, Fernando Seco Granja, José Carlos Prieto Honorato, Jorge I. Guevara Rosas, Accurate pedestrian indoor navigation by tightly coupling foot-mounted IMU and RFID measurements, IEEE Trans. Instrum. Meas. 61 (1) (2012) 178–189.
[24] Wilson Sakpere, Michael Adeyeye Oshin, Nhlanhla B.W. Mlitwa, A state-of-the-art survey of indoor positioning and navigation systems and technologies, South Afr. Comput. J. 29 (3) (2017).
[25] A. Koutsou, F. Seco, A. Jimnez, J. Roa, J. Ealo, J. Prieto, J. Guevara, Preliminary localization results with an RFID based indoor guiding system, Proc. IEEE Int. Symp. Intell. Signal Process. (2007) 917–922.
[26] O. Woodman, R. Harle, RF-based initialisation for inertial pedestrian tracking, Proc. 7th Int. Conf. Pervasive Comput. (2009) 238.
[27] K. Zhang, M. Zhu, G. Retscher, F. Wu, W. Cartwright, Three-dimension indoor positioning algorithms using an integrated RFID/INS system in multi-storey buildings, Proc. Location Based Services Tele Cartography II (2009) 373–386.
[28] Isaac Skog, John-Olof Nilsson, Dave Zachariah, and Peter Handel. Fusing the Information from Two Navigation Systems Using an Upper Bound on Their Maximum Spatial Separation. 2012 International Conference on Indoor Positioning and Indoor Navigation. 2012.
[29] John-Olof Nilsson, Dave Zachariah, Isaac Skog, Peter Händel, Cooperative localization by dual foot-mounted inertial sensors and inter-agent ranging, EURASIP J. Adv. Signal Process. 164 (2013).
[30] J.N. Kim, M.H. Ryu, Y.S. YANG, Detection of gait event and supporting leg during over ground walking with mediolateral swing angle, Innovation Mater. Sci. Emerging Technol. 145 (2011) 567–573.
[31] S. Lambrecht, A.J. Del-Ama, Human movement analysis with inertial sensors, Biosyst. Bio Rob. (2014).
[32] J.-A. Lee, S.-H. Cho, Y.-J. Lee, H.-K. Yang, J.-W. Lee, Portable activity monitoring system for temporal parameters of gait cycles, J. Med. Syst. 34 (2010) 959–966.
[33] S.K. Park, Y.S. Suh, A zero velocity detection algorithm using inertial sensors for pedestrian navigation systems, Sensors 10 (10) (2010) 9163–9178.

[34] I. Skog, J.O. Nilsson, P. Händel, Evaluation of zero-velocity detectors for foot-mounted inertial navigation systems, in: Proc. 2010 Int'l Conf. Indoor Positioning and Indoor Navigation, extended abstract, IEEE, 2010, pp. 172–173.
[35] Nadir Castaneda, Sylvie Lamy-Perbal. An improved shoe-mounted inertial navigation system, in: 2010 International Conference on Indoor Positioning and Indoor Navigation (IPIN). Zurich, Switzerland, Sep. 2010. 15–17.
[36] J. Pinchin, C. Hide, T. Moore. A particle filter approach to indoor navigation using a foot mounted inertial navigation system and heuristic heading information,in: International Conference on Indoor Positioning and Indoor Navigation (IPIN). Sydney, Australia. 2012, 13–15.
[37] Nachi Gupta, Raphael Hauser, Kalman Filtering with Equality and Inequality State Constraints, Oxford University Computing Laboratory, 2008.
[38] Dan Simon, Donald L. Simon, Kalman Filtering with inequality constraints for turbofan engine health estimation, IEEE Proc. Control Theory Appl. (2006).
[39] Yueyang Ben, Guisheng Yin, Wei Gao, Feng Sun, Improved filter estimation method applied in zero velocity update for SINS, 2009 International Conference on Mechatronics and Automation, 2009.
[40] Arvind Ramanandan, Anning Chen, Jay A. Farrell, Observability analysis of an inertial navigation system with stationary updates, Proceedings of the 2011 American Control Conference, IEEE, 2011.